Proceedings World Geothermal Congress 2020+1
Reykjavik, Iceland, April - October 2021

Geothermal Surface Manifestation Characterization Using Airborne Lidar Return Intensity

Yan Restu Freski[1,2], Christoph Hecker[1], Agung Setianto[2], Freek D. van der Meer[1]

[1]ITC Faculty of Geo-Information Science and Earth Observation, University of Twente, The Netherlands

[2]Department of Geological Engineering, Faculty of Engineering, Universitas Gadjah Mada, Indonesia

[1]y.r.freski@utwente.nl

Keywords: LiDAR intensity, airborne laser scanning, geothermal surface manifestation

ABSTRACT

Laser Return Intensity (LRI) holds excellent opportunity in helping to map lithology and discriminating rock units based on their reflectivity. To date, many rock types have been examined under a controlled environment using Terrestrial Lidar Scanning (TLS). However, the utilization of LRI for detection of rocks properties in a geothermal environment still has received less attention especially from Airborne Lidar Scanning (ALS). This study proposes a novel approach to map and characterize geothermal surface manifestations using airborne lidar return intensity. We use an airborne lidar dataset acquired by a Leica ALS70 above the geothermal field near Bajawa, Flores, Indonesia. The effects of scan angle and atmosphere on the resulting LRI images were investigated and where possible corrected for optimizing the positional and spectral information. Characterization of geothermal surface manifestation signatures based on altered volcanic rock reflectivity through LRI were validated by the ground truth observation and airborne thermal infrared imagery in Wawomuda and Mataloko, Bajawa. We will present an overview of the data corrections needed to evaluate the lidar return intensity values for detecting geothermal surface manifestations in the tropical mountainous environment.

1. INTRODUCTION

The Laser Return Intensity (LRI), a value of reflectance detected from a scanned object, has been used for helping detection and mapping lithology as it can sense the physical properties of sedimentary rocks (Clark and Roush, 1984; Clark, 1999; Franceschi *et al.*, 2009; Burton *et al.*, 2011; Penasa *et al.*, 2014; Živec, Anžur and Verbovšek, 2017), igneous and metamorphic rocks (Carrea *et al.*, 2016). These studies used Terrestrial Laser Scanning (TLS) to distinguish rocks from laboratory to outcrop scale, e.g., marls and limestone (Franceschi *et al.*, 2009), chert (Penasa *et al.*, 2014), peridotite, gneiss, serpentinite, mica-schist, and marble (Carrea *et al.*, 2016), clay-rich and quartz-rich sedimentary rocks in a set of drill core and stratigraphic outcrop (Burton *et al.*, 2011).

The texture of rocks influences the value of intensity (Clark, 1981, 1999; Burton *et al.*, 2011) such as grain size and fabric—related to porosity. Even fresh sedimentary rocks are mostly clastic-matrix supported which can contain more water than fresh crystalline rock. This water content can be a proxy of rock texture in the intensity value of most LiDAR dataset, which are produced in visible-near infrared (VNIR) region (Chust *et al.*, 2008; Hartzell *et al.*, 2014; Shi *et al.*, 2015; Yan, Shaker and El-Ashmawy, 2015; Eitel *et al.*, 2016; Errington and Daku, 2017; Budei *et al.*, 2018; Ekhtari, Glennie and Fernandez-Diaz, 2018; Zhao *et al.*, 2018). The water, the photon absorbent (Clark, 1999), will be low value and appeared as dark in the intensity map. On the contrary, fresh crystalline rocks may have a brighter tone in the intensity map as they are often massive unless they have pores with water content.

Many rocks have been scrutinized using LiDAR technology but the rocks from the geothermal process. In a geothermal environment, the rocks ranging from fresh as host rock to fully hydrothermally altered with diverse mineral abundance. Each mineral association indicates an interaction between meteoric-magmatic fluid, heat influx, and geological setting (host rocks and geological structures). Terrain setting where the geothermal system locates also contributes to set up the fluid circulation as a system. This complexity has been classified to describe the geothermal manifestations (Hochstein and Browne, 2000).

We are curious about 'Can the LiDAR intensity characterize and map the geothermal surface manifestations?' We choose this natural product as the target since they are obviously indicating the occurrence of a geothermal system. In a geothermal environment, there is a contradictive hypothesis on intensity response. We assume that most active surface manifestations are wet because the fluid circulates. They will be darker compared to drier land surrounding. However, the surface manifestations are also often brighter in physical color, e.g. white or yellowish ground, that should have a higher value of LRI than surrounding. Therefore, it is an interesting curiosity to see how the LRI reacts to the geothermal surface manifestations, so we can look at the possibility to use the LRI especially from Airborne Laser Scanning (ALS) survey to map and characterize the geothermal surface manifestations.

2. METHODS

This preliminary study proposes an approach to detect and map geothermal surface manifestations using an airborne LiDAR dataset acquired from a geothermal field near Bajawa city, Flores, Indonesia (Figure 1). We will use the ALS dataset collected by Leica ALS70 with wavelength 1064 nm (within the VNIR region) that can approach the moisture variation. The time of LiDAR acquisition was in July when the peak dry season approaching the area. This period was chosen to minimize the cloud thickness as part of atmospheric effect.

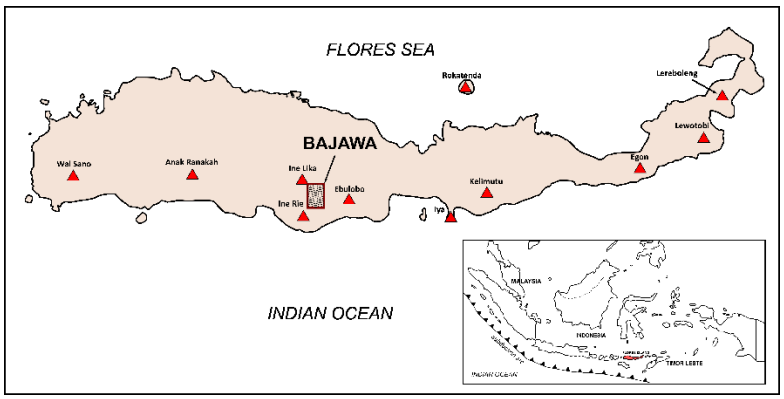

Figure 1: Location of the research area in Bajawa, Flores Island, Indonesia.

First, we will overview the readiness level of data for interpretation (Kashani *et al.*, 2015). This level can lead us to decide which processing is necessary and explain the limitation of interpretation. Hence, some corrections may be needed to minimize the misinterpretation. We will observe and extract the intensity value throughout the dataset. We also will use the x-y-z position as a digital elevation model and its derivative information to support the interpretation especially for indicating the possibility of sun heating influences.

In the case of the geothermal field in Bajawa, the known manifestations are in Wawomuda and Mataloko. They are nested in the aligned monogenetic volcanoes which some of the volcanoes are still active. Therefore, there are hot mud pools and hot springs with and without aerosol coming out from the hydrothermally altered ground. This phenomenon indicates the active geothermal system. The ground truth will be described to verify the behavior of intensity value. Thermal imagery will be used to provide information about heat anomalies. This data can roughly discriminate against the active from fossil manifestations.

Finally, we will decide the possibility of uses of LRI to characterize the geothermal surface manifestation as well as the limitation and challenges.

3. RATIONALES

The hypothesis of this study is that the intensity value of geothermal surface manifestation will be various depending on the moisture of the ground, the amount of aerosol emitted, and the sloping terrain as the incident angle manifestation (as shown in Figure 2). The moisture indicates how much water absorbed within pores. This parameter is related to the textural properties of rock, e.g., grain size and compactness. The amount of aerosol can influence the ability of the laser to reach the ground. The terrain landscape is considered as geometrical factors of the LRI.

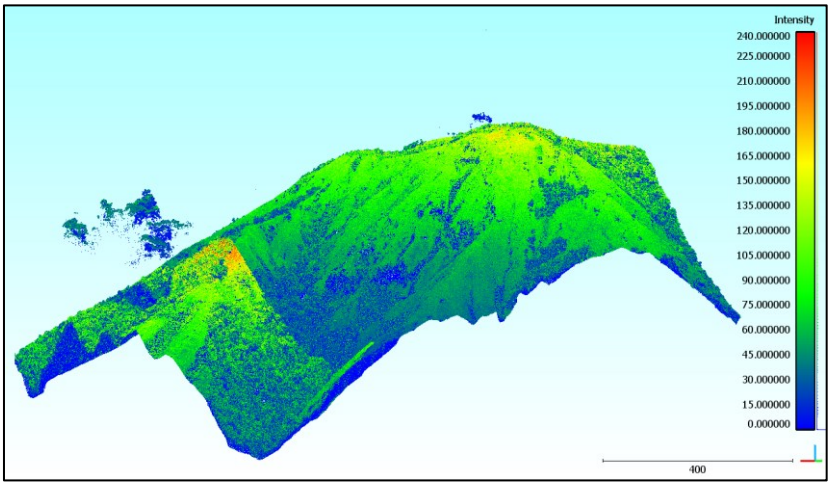

Figure 2: The LRI of an undulating terrain near the geothermal field in Bajawa, Flores. Grading color from blue to red indicates low (digital number 0) to high reflectivity (digital number 240). This figure shows the effect of object moisture, aerosol, and sloping terrain. Objects with high moisture (blue) are the area with high level of vegetation and cloud while drier object (green to yellow) is the land covered by low level of vegetation. A floating-point cloud on the right side above the terrain is atmospheric cloud, which blocks the laser signal from aircraft to ground and vice versa (low reflectivity of the ground under the cloud). The upper ridges reflect the laser signal stronger than the gullies as the effect of terrain.

3.1 Moisture of rock

The value of LRI can be influenced by textural properties, e.g., grain size (Kaasalainen *et al.*, 2011; Nield, King and Jacobs, 2014). Grain size is related to the degree of porosity and permeability. The pores within the rock may be connected and contain more water. Hence, the LRI of wet rocks is lower than of drier rocks (Nield, King and Jacobs, 2014). Grain size can contribute to the porosity

where the smaller size of grains generally will build a high volume of pores. In most clay-size-grained rocks, the permeability is much lower than coarser-grained. For instance, clay-size-grained rock will tend to absorb more water and need more times to dry than the coarser-grained rock since the porosity is greater but impermeable. However, it is still possible to have a coarse-grained rock with high moisture.

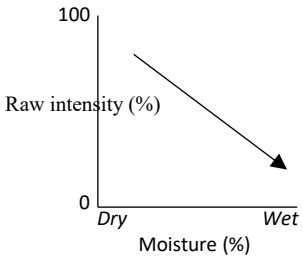

Figure 3: Hypothetical trend of LRI value on moisture.

The freshness of rocks means the degree of alteration caused by the hydrothermal process or meteoric weathering. Compactness is the extended parameter of rock freshness where the fresh rock will be always more compact than the altered rock. The previous experiment of grain size (Kaasalainen *et al.*, 2011) and moisture (Nield, King and Jacobs, 2014) did not discuss the LRI response on the degree of alteration.

3.2 Aerosol effect

The aerosol emitted from the manifestation is mainly steam or water vapor which can block the laser from reaching the ground. It may absorb the photon of the laser and allow a smaller quantity of the photon to pass. The penetrated photon then reflected by the ground with a smaller amount. Since the aerosol of manifestations is produced continuously above the ground, the very small photons of laser are absorbed again. Thus, the aerosol attenuates the intensity value on the ground.

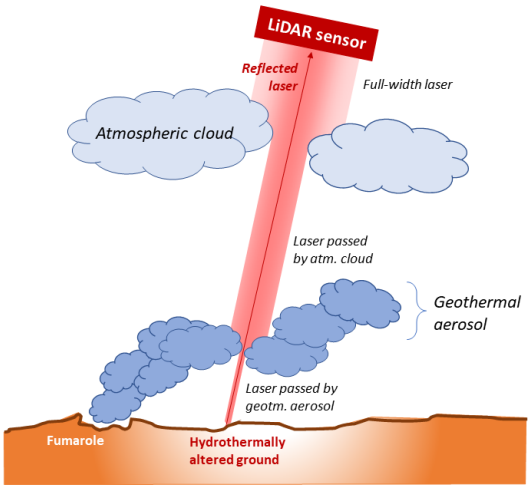

Figure 4: Attenuating value of LRI due to aerosol in the atmosphere and from fumarole. Note that the reflected laser is not always in the center of a footprint

The aerosol also can be an atmospheric cloud covering the land. Moreover, the study area is mountainous terrain with hundreds of meters above sea level. This aircraft Pilatus PC 6 used in the acquisition was flown ± 800 m above average ground level. Above this maximum height, the laser will against thick cloud while lower than that, the scanned swath will be narrower. Consequently, the point density also will not be uniformly collected which can spatially impact the data quality.

The atmospheric cloud was dynamic through the time of acquisition. Therefore, different flight height might happen to avoid the cloud. It might cause a different range in the intensity value each scan line since each scanning will collect the intensity arbitrarily in digital number format from 0 to 255. The different flight height also influences the footprint size of the laser beam. With 800 m above ground level, it is reported that the footprint size was ± 10 cm. The larger footprint will tend to be less accurate than the smaller one as larger footprint will take more characters of ground into only one value.

3.3 Terrain effect

The mountainous terrain in Bajawa with a diverse degree of slope provide the various incident angle. Following the rule of the Lambertian angle, the small angle of incidence may yield a high value of LRI. The flatter ground will be more reflective. Corresponding the incident angle, the range effect will also influence the LRI. The value of LRI in the ridges area will be higher than on gullies or valleys. Besides the ridges are closer to the scanning sensor, it is also flatter.

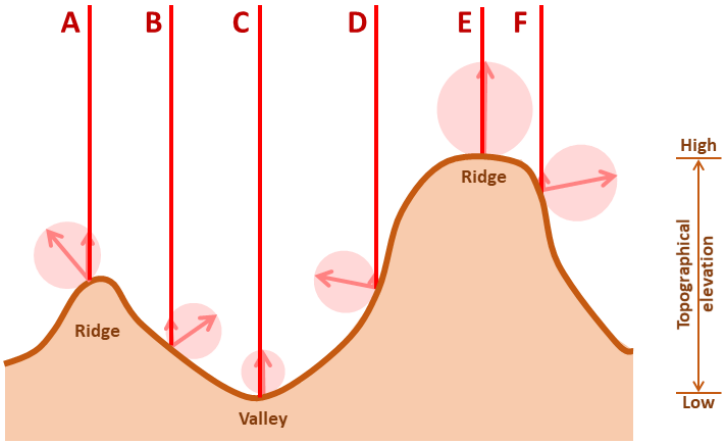

Figure 5: Terrain effects are functions of topographical elevation and slope degree. Note that circles show the reflectance value due to Lambertian rule. The topographical elevation represents the range effect between scanning sensor and ground. Laser E reaches the closer ground (higher elevation) than laser C, then the reflected laser E is greater than C. Laser A-B-D-F shows the smaller value of intensity will be reflected compared to the specular vector.

4. CONCLUSION

Theoretically, geothermal manifestations are possible to be detected using lidar return intensity values from Airborne Lidar Scanning (ALS) dataset. The minimum corrections for LRI data acquired from a tropical-mountainous terrain environment should accommodate the intensity variation caused by the effect of moisture, aerosol, and the incidence angle due to the terrain slope. The challenges also can come from the technical factor e.g., the acquisition process, and the object characteristic factor e.g., the mixing condition of wetness and brightness of ground.

REFERENCES

Budei, B. C. *et al.* (2018) 'Identifying the genus or species of individual trees using a three-wavelength airborne lidar system', *Remote Sensing of Environment*. Elsevier, 204(September 2017), pp. 632–647. doi: 10.1016/j.rse.2017.09.037.

Burton, D. *et al.* (2011) 'Lidar intensity as a remote sensor of rock properties', *Journal of Sedimentary Research*. SEPM Society for Sedimentary Geology, 81(5), pp. 339–347. doi: 10.2110/jsr.2011.31.

Carrea, D. *et al.* (2016) 'Correction of terrestrial LiDAR intensity channel using Oren–Nayar reflectance model: An application to lithological differentiation', *ISPRS Journal of Photogrammetry and Remote Sensing*. Elsevier, 113, pp. 17–29. doi: 10.1016/j.isprsjprs.2015.12.004.

Chust, G. *et al.* (2008) 'Coastal and estuarine habitat mapping, using LIDAR height and intensity and multi-spectral imagery', *Estuarine, Coastal and Shelf Science*, 78(4), pp. 633–643. doi: 10.1016/j.ecss.2008.02.003.

Clark, R. N. (1981) 'The spectral reflectance of water-mineral mixtures at low temperatures', *Journal of Geophysical Research: Solid Earth*, 86(B4), pp. 3074–3086. doi: 10.1029/JB086iB04p03074.

Clark, R. N. (1999) 'Spectroscopy of rocks and minerals, and principles of spectroscopy', in Rencz, A. N. (ed.) *Manual of Remote Sensing, Remote sensing for the Earth Sciences*. 3rd edn. New York: John Wiley and Sons, pp. 3–58.

Clark, R. N. and Roush, T. L. (1984) 'Reflectance spectroscopy: Quantitative analysis techniques for remote sensing applications', *Journal of Geophysical Research: Solid Earth*, 89(B7), pp. 6329–6340. doi: 10.1029/JB089iB07p06329.

Eitel, J. U. H. *et al.* (2016) 'Beyond 3-D: The new spectrum of lidar applications for earth and ecological sciences', *Remote Sensing of Environment*, 186, pp. 372–392. doi: 10.1016/j.rse.2016.08.018.

Ekhtari, N., Glennie, C. and Fernandez-Diaz, J. C. (2018) 'Classification of airborne multispectral lidar point clouds for land cover mapping', *IEEE Journal of Selected Topics in Applied Earth Observations and Remote Sensing*. IEEE, 11(6), pp. 2068–2078. doi: 10.1109/JSTARS.2018.2835483.

Errington, A. and Daku, B. (2017) 'Temperature Compensation for Radiometric Correction of Terrestrial LiDAR Intensity Data', *Remote Sensing*, 9(4), p. 356. doi: 10.3390/rs9040356.

Franceschi, M. *et al.* (2009) 'Discrimination between marls and limestones using intensity data from terrestrial laser scanner', *ISPRS Journal of Photogrammetry and Remote Sensing*. Elsevier B.V., 64(6), pp. 522–528. doi: 10.1016/j.isprsjprs.2009.03.003.

Hartzell, P. *et al.* (2014) 'Application of multispectral LiDAR to automated virtual outcrop geology', *ISPRS Journal of Photogrammetry and Remote Sensing*. International Society for Photogrammetry and Remote Sensing, Inc. (ISPRS), 88(5), pp. 147–155. doi: 10.1016/j.isprsjprs.2013.12.004.

Hochstein, M. P., and Browne, P. R. L. (2000) 'Surface manifestations of geothermal systems with volcanic heat sources', in H, S. (ed.) *Encyclopedia of volcanoes*. New York: Academic, pp. 835–55.

Kaasalainen, S. *et al.* (2011) 'Analysis of incidence angle and distance effects on terrestrial laser scanner intensity: Search for correction methods', *Remote Sensing*, 3(10), pp. 2207–2221. doi: 10.3390/rs3102207.

Kashani, A. G. *et al.* (2015) 'A review of LIDAR radiometric processing: From ad hoc intensity correction to rigorous radiometric calibration', *Sensors (Switzerland)*, 15(11), pp. 28099–28128. doi: 10.3390/s151128099.

Nield, J. M., King, J. and Jacobs, B. (2014) 'Detecting surface moisture in aeolian environments using terrestrial laser scanning', *Aeolian Research*. Elsevier B.V., 12, pp. 9–17. doi: 10.1016/j.aeolia.2013.10.006.

Penasa, L. *et al.* (2014) 'Integration of intensity textures and local geometry descriptors from Terrestrial Laser Scanning to map chert in outcrops', *ISPRS Journal of Photogrammetry and Remote Sensing*. International Society for Photogrammetry and Remote Sensing, Inc. (ISPRS), 93, pp. 88–97. doi: 10.1016/j.isprsjprs.2014.04.003.

Shi, S. *et al.* (2015) 'Improving Backscatter Intensity Calibration for Multispectral LiDAR', *IEEE Geoscience and Remote Sensing Letters*, 12(7), pp. 1421–1425. doi: 10.1109/LGRS.2015.2405573.

Yan, W. Y., Shaker, A. and El-Ashmawy, N. (2015) 'Urban land cover classification using airborne LiDAR data: A review', *Remote Sensing of Environment*. Elsevier Inc., 158, pp. 295–310. doi: 10.1016/j.rse.2014.11.001.

Zhao, H. *et al.* (2018) 'A method of determining multi-wavelength lidar ratios combining aerodynamic particle sizer spectrometer and sun-photometer', *Journal of Quantitative Spectroscopy and Radiative Transfer*. Elsevier Ltd, 217, pp. 224–228. doi: 10.1016/j.jqsrt.2018.05.030.

Živec, T., Anžur, A. and Verbovšek, T. (2017) 'Using the Intensity Values from Terrestrial Laser Scanner (TLS) for Determining Lithology of Flysch Rock Mass in Southwest Slovenia', in Mikoš, M. et al. (eds) *Advancing the culture of living with landslides*. Cham: Springer, pp. 201–207. doi: 10.1007/978-3-319-53483-1.